Prediction of Rupture Using Ductile and MSFLD Damage in T-Shape Tube Hydro-Forming Process

H. Ghazavi*
Department of Mechanical Engineering,
Najafabad Branch, Islamic Azad University, Isfahan, Iran
E-mail:hosseingh_info@yahoo.com
***Corresponding author

N. Solhjoei
Department of Mechanical Engineering,
Najafabad Branch, Islamic Azad University, Isfahan, Iran
E-mail: solhjoei@yahoo.com

Received: 13 November 2011, Revised: 10 December 2011, Accepted: 20 December 2011

Abstract: Hydro-forming is a fabrication process that uses a fluid mediumto form a component by using high internalpressure. In tube hydro-forming, a tubular blank is placed between two dies, sealed and pressurized water injected, deforming the tube walls in the forming cavity of the dies. Several typical hydro-forming processes such as T- shapes, cross-shapes and Y- shapes exist. Successful hydro-forming depends on selection of proper tubular blank, sound preformed shape and internal pressure. In this paper, a 3D model of hydro-forming process of a T-shaped tube has been simulated by finite element method. Two damage models, coupled with von Mises plastic criterion, have been applied to predict where and when ductile and MSFLD rupture occur in the process. All studies presented in this paper have been carried out on aluminium alloy EN AW-7108 T6**.**

Keywords: Aluminium Alloy ENAW-7108-T6, Ductile Fracture Criteria, Finite Element Simulation, Hydro-Forming, MSFLD Fracture Criteria, T-shape Tube,

Reference: Ghazavi, H. and Solhjoei, N., 'Prediction of Rupture Using Ductile and MSFLD Damage in T- Shape Tube Hydro-Forming Process', Int J of Advanced Design and Manufacturing Technology, Vol. 5/No. 3, 2012, pp. 53-60.

Biographical notes: H. Ghazavi received his Bachelor in Mechanical Engineering from University of IAU Najafabad Branch, in 2008. He is Master Student ofMechanical Engineering at IAU, Najafabad Branch, Isfahan, Iran. His current research interest includes flow-forming, spinning, hydro-forming, and deep-drawing. **N. Solhjoei**is Associate Professor in Mechanical engineering department at the University of Najafabad, Iran. He received his PhD in Mechanical engineering from France. His current research focuses on fluid mechanics, thermodynamics and dynamics.

1 INTRODUCTION

Hydro-forming is a process for manufacturing complex hollow components, in most cases using circular tubes as a source material. To manufacture a hydro-formed component, a circular tube is inserted into a suitable die, sealed on both sides by two horizontal cylinders, and is subsequently formed to conform to the shape of the die cavity by internal hydraulic pressure. Compared to conventional forming processes, hydro-forming process has the potential of offering significant reductions in piece cost, tool cost, and weight for many automotive body and chassis applications. Therefore, this young technology is currently prevalent in automotive and aircraft industries, as well as in the manufacturing components for sanitary industry.It is expensive and time consuming to design the process using trial and error for the hydro-forming process, as well as the conventional forming process. The application of numerical simulation for the hydro-forming process will help engineers to efficiently improve the process development [1]. Due to the complexity of the hydro-forming process, theoretical studies to date have produced a relatively limited understanding of the process. In comparison with other theoretical methods, the finite element method (FEM) has advantages in solving general problems with formed parts having complex shapes [2].Until now, several finite element simulation studies on hydro-forming process have been reported in literature. Most FEM simulation results for hydro-forming process have been carried out by dynamic explicit FEM packages, which have the advantage of fast changing boundary conditions for complex die surfaces. Even though the implicit FEM provides a more reliable and rigorous scheme in considering the equilibrium at each step of deformation, the major obstacle for the implicit FEM lies in cases for which converged solutions cannot be found because of the changing contact and friction conditions at arbitrary tool shapes, and longtime consumption to handle contact conditions [3]. Simulation results for hydro-forming processes using implicit FEM package were usually limited to simple die geometries. Simulation results provide detailed knowledge on metal flow during the forming process, which allows us to control metal flow and provides a better design strategy in the actual forming process [4].

2 DUCTILE AND MSFLDDAMAGE MODEL

Ductile criterion

The ductile criterion is a phenomenological model for predicting the onset of damage due to nucleation, growth, and coalescence of voids. The model assumes that the equivalent plastic strain at the onset of damage, ε_D^{-pl} is a function of stress triaxiality and strain rateaccording to Eq. (1),

$$\varepsilon_D^{-pl}(\eta, \dot{\varepsilon}^{-pl}) \tag{1}$$

where $\eta = -p/q$is the stress triaxiality, p is the pressure stress, q is the Mises equivalent stress, and $\dot{\varepsilon}^{-pl}$is the equivalent plastic strain rate. The criterion for damage initiation is met when the following condition according to Eq. (2), is satisfied [5].

$$\omega_D = \int \frac{d\varepsilon^{-pl}}{\varepsilon_D^{-pl}(\eta,\dot{\varepsilon}^{-pl})} = 1 \tag{2}$$

whereω_D is a state variable that increases onotonically with plastic deformation. At each iteration during the analysis, the incremental step in $\omega_D$according to Eq. (3) is,

$$\Delta\omega_D = \frac{\Delta\varepsilon^{-pl}}{\varepsilon_D^{-pl}(\eta,\dot{\varepsilon}^{-pl})} \geq 0 \tag{3}$$

For ductile fracture, it is assumed that the equivalent fracture strain$\varepsilon_{eq}^{**}$is a function of the stress triaxialityη, defined in Eq. (4), by components in principal stress.

$$\eta = \frac{3\sigma_m}{\sigma_{eq}} \tag{4}$$

Typically, the dependence of the equivalent fracture strain on the stress triaxiality is expressed in the form of Eq. (5)

$$\varepsilon_{eq}^{**} = d_0 \exp(-c\eta) \tag{5}$$

Equation (5), assumes a monotonic decrease of the fracture strain with increasing stress triaxiality. However, experimental results from used aluminum extrusions show equivalent plastic strain at fracture. Equibiaxial stress ($\eta \cong 2$) can be higher than the equivalent plastic strain at fracture in plane strain loading ($\eta \cong \sqrt{3}$). Equation (6), represents a more general formulation and includes a non-monotonic decrease of the fracture strain with increasing stress triaxiality[6-7].

$$\varepsilon_{eq}^{**} = d0\ exp(-c\eta) + \mathrm{d1}\exp(\mathrm{c\eta}) \tag{6}$$

where$d1$ is an additional material parameter. Of course, Eq. (6) includes aspecial case of Eq. (5), for a monotonic decrease in fracture strain vs. stress triaxiality. However, Eq. (5), and Eq.(6),remain limited to describing isotropic materials. A more general

formulation of Eq. (6), which includes the orthotropy of fracture, must also include the boundary conditions of the equivalent fracture strain ε_T^+ for the equibiaxial tension condition which must not be orientation dependent. Theoretically, the fracture strain at equibiaxial compression ε_T^-must not be orientation dependent as well. However, its value is usually very high. If η^+ is the stress triaxiality for equibiaxial tension and η^- indicates the stress triaxiality in equibiaxial compression (a material with isotropic plasticity yields $\eta^+ = 2$ and $\eta^- = -2$), the following boundary conditions may be definedaccording to Eq. (7), [5].

$$\varepsilon_T^+ = \varepsilon_{eq}^{**} for \eta = \eta^+ \quad (7\text{-a})$$

$$\varepsilon_T^- = \varepsilon_{eq}^{**} for \eta = \eta^- \quad (7\text{-b})$$

The parameters $d0$ and $d1$ of Eq. (6), can be substituted using the boundary conditions from Eqs.(7a) and(7b). The result is given in Eq. (8),

$$\varepsilon_{eq}^{**} = \frac{\varepsilon_T^+ \sinh[c(\eta^- - \eta)] + \varepsilon_T^- \sinh[c(\eta - \eta^+)]}{\sinh[c(\eta^- - \eta^+)]} \quad (8)$$

An orientation dependent parameter c has been introduced in Eq. (8), for the orthotropic case. Therefore Eq. (8) has two constant parameters, $\varepsilon_T^+, \varepsilon_T^-$ and one orientation dependent parameter c. The dependence of the parameter c on the angle $v$between the extrusion direction and the direction of the first principal strain rate$\dot{\varepsilon}_1$ is expressed in Eq. (9),[7].

$$c = k_0 + k_1 cos(2v) + k_2 cos(4 \quad (9)$$

Equations (9) and (10) fulfill the necessary symmetry boundary conditions. Equations (8) and (9) are used to approximate the ductile fracture curve in this paper. The parameter ε_T^+can be directly obtained from anequibiaxial tension test (i.e. Erichsen test). The parameters ε_T^- and c for one direction (extrusion direction) can be derived from two additional experiments with different stress triaxiality. For two different orientations (45°and 90°) the value of c is derived from three point bending tests. If c is known for three orientations (i.e. $c0$, $c45$ and $c90$), the coefficients $k0$, $k1$ and $k2$ of equation (9) can be calculated using equations (10a-c).

$$k0 = (c0 + 2c45 + c90)/4 \quad (10\text{-a})$$

$$k1 = \frac{c0 - c90}{2} \quad (10\text{-b})$$

$$k2 = \frac{c0 - 2c45 + c90}{4} \quad (10\text{-c})$$

Ductile fracture limit curves $\varepsilon_T^{**}(\eta)$areshown in Fig. 1,[8].

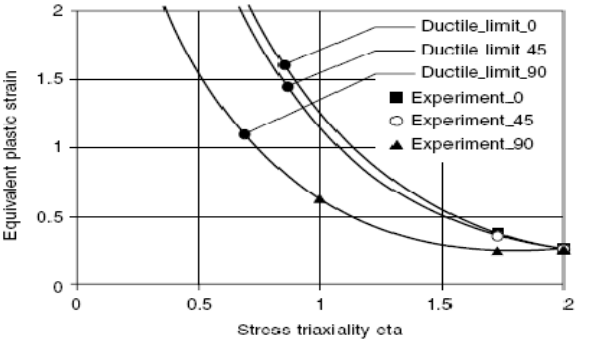

Fig. 1 Ductile fracture limit curves $\varepsilon_T^{**}(\eta)$ compared with experimental data for quasi-static case in orientation of 0°, 45°and 90°to extrusion direction

Muschenborn-sonne forming limit diagram (MSFLD) criterion

Müschenborn and Sonne (1975) proposed a method to predict the influence of the deformation path on the forming limits of sheet metals on the basis of the equivalent plastic strain, by assuming that the forming limit curve represents the sum of the highest attainable equivalent plastic strains. This paper makes use of a generalization of this idea to establish a criterion of necking instability of sheet metals for arbitrary deformation paths. The approach requires transforming the original forming limit curve (without pre-deformation effects) from the space of major versus minor strains to the space of equivalent plastic strain, ε^{-pl} , versus ratio of principal strain rates,$\alpha = \dot{\varepsilon}_{minor}/\dot{\varepsilon}_{major}$
Forming limit curve MSFLDis illustrated in Fig (2), [8].

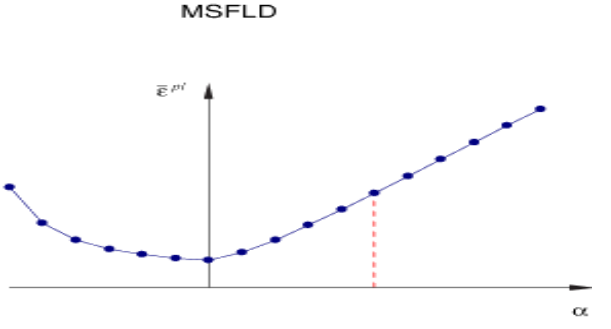

Fig. 2 Forming limit curve for MSFLD

According to the MSFLD criterion, the onset of localized necking occurs when the sequence of deformation states in the $\varepsilon^{-pl} - \alpha$ diagram intersects the forming limit curve, as discussed below. For

arbitrary loading, however, the MSFLD representation takes into account the effects of the history of deformation through the use of the accumulated equivalent plastic strain. For the specification of the MSFLD damage initiation criterion, we can directly provide the equivalent plastic strain at damage initiation as a tabular function of $\alpha$and, optionally, equivalent plastic strain rate, temperature, and predefined field variables, $\varepsilon^{-pl}_{MSFLD}(\alpha, \dot{\varepsilon}^{-pl}, \theta, f_i)$. Let ω_{MSFLD}represent the ratio of the current equivalent plastic strain, $\dot{\varepsilon}^{-pl}$ to the equivalent plastic strain on the limit curve evaluated at the current values of α; strain rate, $\dot{\varepsilon}^{-pl}$;temperature,θ; and predefined field variables, f_i:according to Eq. (11), [5]

$$\omega_{MSFLD} = \frac{\varepsilon^{-pl}}{\varepsilon^{-pl}_{MSFLD}(\alpha,\dot{\varepsilon}^{-pl},\theta,f_i} \tag{11}$$

The MSFLD criterion for necking instability is met when the condition $\omega_{MSFLD} = 1$ is satisfied. Necking instability also occurs if the sequence of deformation states in the $\varepsilon^{-pl} - \alpha$ diagram intersects the limit curve due to a sudden change in the straining direction. This situation is illustrated in Fig. 3. As α changes from α_t to $\alpha_{t+\Delta t}$, the line connecting the corresponding points in the $\varepsilon^{-pl} - \alpha$ diagram intersects with the forming limit curve. When this situation occurs, the MSFLD criterion is reached despite the fact that

$$\varepsilon^{-pl}_{t+\Delta t} < \varepsilon^{-pl}_{MSFLD}(\alpha_t + \Delta_t). \tag{12}$$

Fig. 3, illustrates how a sudden change in the straining direction, from $\alpha_t$to $\alpha_t + \Delta_t$, can produce a horizontal intersection with the limit curve and lead to onset of necking. [6].

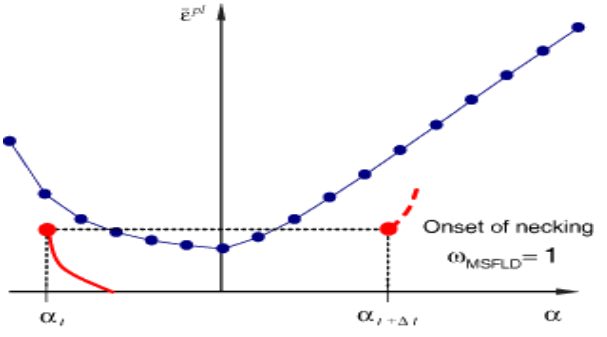

Fig. 3 Sudden change in the straining direction, from $\alpha_t$to $\alpha_t + \Delta_t$

3 MATERIAL PROPERTIES

The material properties used in the simulations are summarized in Table 1. Because the use of aluminum alloy will bring great improvement in weight reduction, now aluminum alloy enjoys wide application in automobile industry. However, due to the low formability of aluminum material, it is more difficult to form aluminum alloy than to form steel [8].

Table 1 Material properties of aluminum alloy EN AW-7108 T6

Density, ρ (kg/m^3)	2700
Young modulus, E (Gpa)	70
Poisson coefficient, ν	0.33
Initial yield stress ,σ_{y0} (Mpa)	311
Yield stress,σ_y (Mpa)	$511.5(0.012 + \varepsilon_{eq})^{0.1148}$
Damage parameter $\varepsilon^+{}_T$	0.26
Damage parameter $\varepsilon^-{}_T$	193
Damage parameter c	1.908

4 FE SIMULATION OF TUBE HYDROFORMING

Fig.4shows geometry and FEM model of the T-shaped tube hydro-forming in which a counter punch is used for controlling the branch shape. Because of symmetry only one half of the die, counter punch and tube were modeled [9].

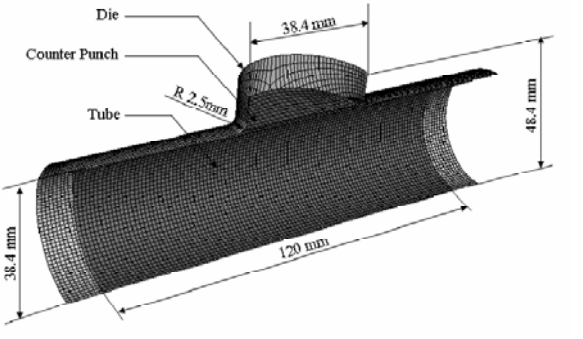

Fig. 4 Finite element modeling of hydro-forming a T-shaped tube

The reason for the interest in computer modeling of the tube hydro-forming processes is mainly economical. Since the majority of tube hydro-forming processes require high pressures, it is not possible to perform try-outs using soft tooling. All the try-outs are performed on hard tooling to verify the process control parameters such as internal pressure and axial feed variations in time. If major modifications are required on tooling after it is manufactured it will be very costly and time consuming. Therefore, computer simulations are increasingly used to verify and fine tune the initial design before the hard tooling is built [10],[11].

Various software packages available in the world market are capable of simulating the tube hydro-forming process. Explicit and implicit programs are available. For hydro-forming, it is important to use a code, which is capable of describing "follower forces". A simple definition of a follower force is a load that must be able to follow the deformed geometry, which means that the pressure must always be perpendicular to the actual part geometry. Pressure is usually described by a pressure-time function but this may cause stability problems in some cases. However, using a flowing volume–time function (of the pump) instead of a pressure–time function eliminates the stability problem [12].

5 FINITE ELEMENT MODEL

In this paper, the explicit FE code is used to simulate the tube hydro-forming. The reason for using explicit code is that ABAQUS software can show the bending and unbending effects of the tube wall on the tube forming. ABAQUS is a famous software which can be used in the research field of hydro-forming. Two calculation methods including dynamic explicit and static implicit can be used in this software. In this paper, the dynamic explicit method has been used.

Due to the characteristic of axis-symmetry, only half a model was selected during the numerical simulation. The tools including die cavity and punches were modeled as rigid elements and the tube blank as von Mises material with 200 elements in the axial direction. The applied material model has elastic–plastic behavior with isotropic and kinematic hardening which does not take the Bauschinger effect into consideration. It is assumed that the static friction coefficient equals the dynamic friction coefficient.

Using the Coulomb friction law, the friction coefficients between tools and blank are 0.05 which is the same as in the experiment. Tube thickness was assumed 1 mm. The penalty method algorithm was used for contact with friction coefficient of 0.05. By using a counter punch, formation of the branch can be improved due to a better control of the material movement in the branch. With axial feed of 15 mm and applied internal fluid pressure of 125 MPa, the tube is formed perfectly and a sound T-shaped joint with a branch of 10 mm length is made.Loading path, i.e. internal pressure vs. axial feeding was assumed as shown in Fig. 5. The loading path consists of two stages. In the first stage, internal pressure and axial feeding increase until one third of the axial feeding is applied. In the second stage, internal pressure increases more slowly in comparison with the first stage.

6 FRICTION

Lubrication and friction conditions in hydro-forming are very critical especially in parts where substantial axial feeding is required. In such cases, lubricant is used to reduce the sliding friction and prevent sticking and galling to reduce tool wear, axial forces and buckling lubrication also becomes a critical factor during the calibration stage when tube cross-section is stretch formed to the final dimensions [13],[14]. As soon as the tube surface is in contact with the die, a friction interface is generated, and depending on the level of friction, the strain distribution will not be uniform any more. Material will be locally stretched to form the final shape.

In order to distribute the stretching over a broader section of the tube, friction should be low, and thus, material should be allowed to flow into the deformation zone [15]. In hydro-forming, boundary lubrication governs the friction conditions. The lubricant trapped between the asperities on the tube and die surfaces provide the lubrication. As the internal pressure increases, contact area at the interface increases and sticking friction may occur. Therefore, under various pressure conditions, different friction laws may be used to model the friction conditions. At low pressures, Coulomb friction may be used. According to the Coulomb friction law, the tangential (frictional) stress (τ) is proportional to the normal stress (σ) at the interface. The proportionality constant is called the friction coefficient (μ). If the contact pressure is close to the flow stress of the tube material, then, the Coulomb friction model does not apply anymore, and the Shear Stress model needs to be used. According to the Shear Stress model, the tangential (frictional) stress (τ) at the interface is proportional to the flow stress [16], [17].The proportionality constant is called the friction factor (f). In this paper, friction coefficient of μ = 0.05 was regarded as a good lubrication at the interface tube-tooling.

7 DETERMINATION OF LOADING PATH

Not only the success of achieving a completely formed hydro-formed part but also the success of forming the part with required thickness specifications is dependent on the selection of an appropriate loading path for already selected set of material, lubrication and part and tooling design [18]. Proper coordination of internal pressure and axial feeding is the key issue as these process parameters have to be applied synchronously. Loading path, i.e. internal pressure vs. axial feeding was assumed as shown in Fig. 5.

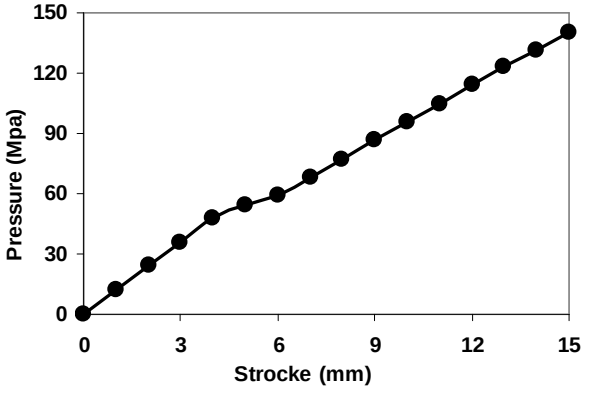

Fig. 5 Loading path

Many process parameters influence tube forming, where the main parameters are internal pressure and the punch stroke. How the optimum values between internal pressure and the punch stroke are found is the key point during tube forming process.

8 KEY POINTS

During tube hydro-forming, the main failure types are buckling, harmful wrinkles, folding back and fracture. It is important to control the material flow during forming so that the failure types will not emerge and the wall thickness reduction can be kept within limitations. Many process parameters influence the tube hydro-forming, the main parameters are the internal pressure P_s and the punch stroke P_t. How to find the optimum values between internal pressure and the punch stroke is one of the key points. Generally, the process windows should be created in both the pre-forming stage and the calibration stage. Both in the pre-forming stage and in the calibration stage, the loading path for internal pressure P_s versus punch stroke P_t can normally be divided into the following two types: (1) the first type is named two-steps or multi-steps variation method. When the punch moves forward, the internal pressure P_f (feeding pressure) keeps no change, which can be called the first step. Then the internal pressure will be increased as high as possible to flatten the useful wrinkles formed in the former period, which can be called calibration pressure P_c in the second step; (2) the second type is named the linear variation method. When the punch moves forward, the internal pressure increases linearly[19], [20], [21].

9 RESULTS AND DISCUSSION

Initially the simulation parameters were chosen such that a sound and defect free part can be made. In other words the process could be done without any defects like buckling, wrinkling, necking, crack and rupture. Result and overall deformed shape of the aluminum obtained from the hydro-forming simulation is shown in Fig. 6.

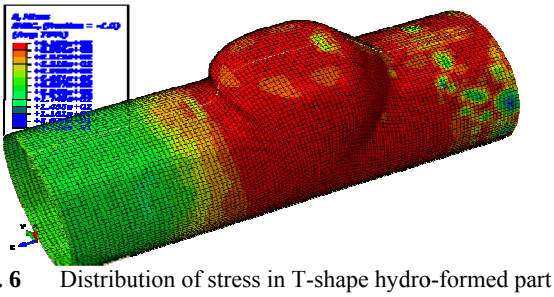

Fig. 6 Distribution of stress in T-shape hydro-formed part without rupture

Fig. 7 shows finite element result that is in good agreement with experimental test.

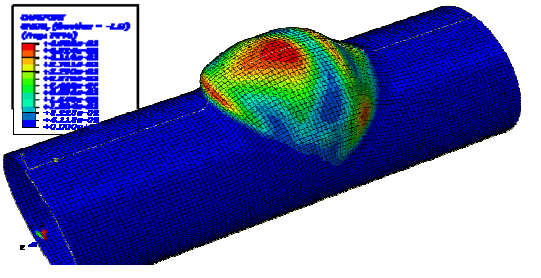

Fig. 7 Result of FE simulation in T-shape hydro-formed part without rupture

In this case, maximum magnitude of observed ductile damage variable was 0.493 at the end of the process, which means that according to this simulation, fracture will not occur. Experimental test was performed with the same forming conditions and an undamaged part was produced. Fig. 8 shows result of experimental test in T-shape hydro-formed part without rupture.

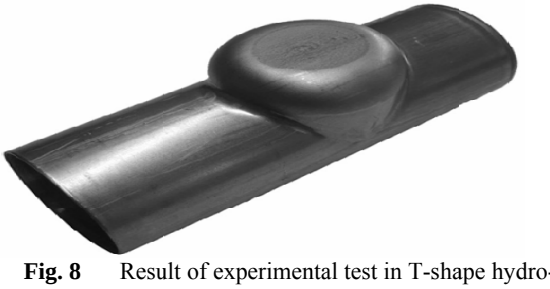

Fig. 8 Result of experimental test in T-shape hydro-formed part

Now, internal pressure and axial feeding increase monotonically. Damage growth variable was studied to predict instance and location of ductile fracture in the forming tube. By using the loading path, damage

increases and with its growth, crack and ductile and MSFLD fracture is observed. Result and overall deformed shape of the aluminum obtained from the hydro-forming simulation is shown in Fig. 9. Fig. 10 shows predicted results of damage growth contours and position of crack and ductile rupture.

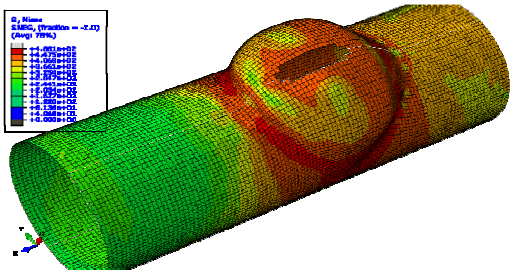

Fig. 9 Distribution of stress in T-shape hydro-formed part with ductile fracture criteria

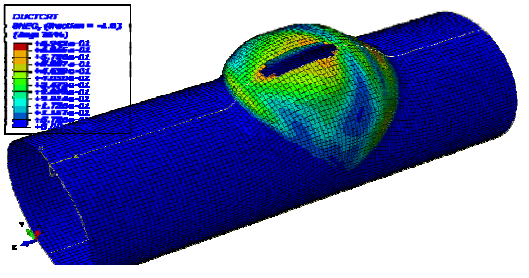

Fig. 10 Prediction of T-shape hydro-formed part with ductile fracture criteria

In this case, maximum magnitude of observed ductile damage variable was 0.692 at the end of the process, which means that according to this simulation, fracture will occur. Fig. 11 shows the result of experimental test in T-shape hydro-formed part with rupture.

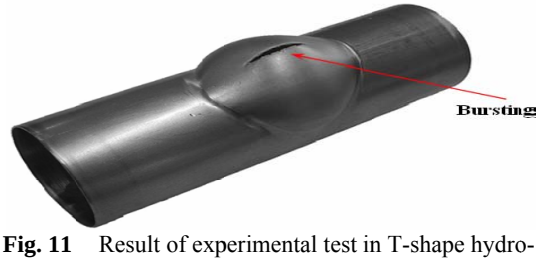

Fig. 11 Result of experimental test in T-shape hydro-formed part with ductile damage

Experimental test was performed with the same forming conditions and a damaged part was produced. Fig.10 shows finite element result that is in good agreement with experimental test. Fig. 12 shows distribution of stress and Fig. 13 shows prediction of T-shape hydro-formed part with MSFLD fracture criteria.

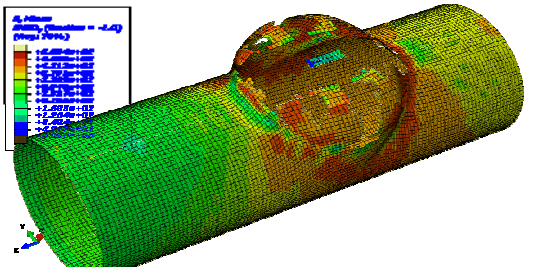

Fig. 12 Distribution of stress in T-shape hydro-formed part with MSFLD fracture criteria

In this case, maximum magnitude of observed ductile damage variable was 0.695 at the end of the process, which means that according to this simulation, fracture will occur. It is realized that ductile damage model can be applied as a proper criterion to determine forming limits and prediction of ductile fracture.

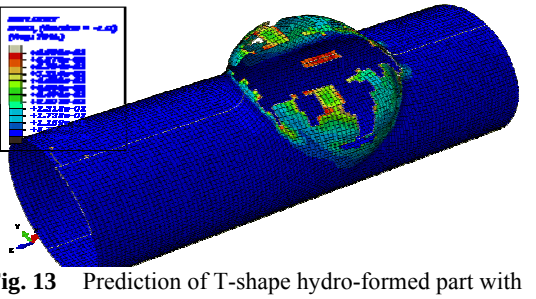

Fig. 13 Prediction of T-shape hydro-formed part with MSFLD fracture criteria

In this case, maximum magnitude of observed ductile damage variable was 0.695 at the end of the process, which means that according to this simulation, fracture will occur. It is realized that ductile damage model can be applied as a proper criterion to determine forming limits and prediction of ductile fracture.

10 CONCLUSION

All studies presented in this paper were carried out on extrusions made from aluminum alloy EN AW-7108 T6. Comparison of numerical results to test data for the hydro-forming demonstrates a comprehensive approach to accurately predict component failure, both in terms of the mode and the location of cracks .The numerical approach based on the FEM provides the information on the forming process, and predicts the effects of process parameters. Thus the potential of hydro-forming process can be dramatically improved with this information by reducing trial and error in tool and process design. The simulation results provide insight and understanding during the actual design and will benefit the development and application of hydro-

forming process to a wide range of applications. Using a ductile damage model coupled with von Mises criterion, time and location of crack onset and ductile rupture in the process was predicted by the FEM. Numerical results of critical failure areas were compared with experimental observations. Also it is realized that ductile damage model can be applied as a proper criterion to determine forming limits and predict ductile fracture in complex and complicated hydro-forming operations.

For tube hydro-forming the formability of the tube hydro-forming is strongly dependent on the loading paths, indicating that the end feeding condition has a definite effect on the onset of bursting. The hydro-forming of T-shapes requires proper selection of many process parameters, i.e. the internal pressure, the axial feeds (at the left and right ends), and the counter punch force. All these parameters are crucial to the success of the hydro-forming operation.

REFERENCES

[1] Liang, X. and Tomasz, W., "Ductile fracture initiation and propagation modeling using damage plasticity theory", Journal of engineering fracture mechanics, Vol. 75, No. 1, 2008. pp. 3276–3293

[2] Hill, R., "On discontinuous plastic states with special reference to localisednecking in thin sheets", Journal. of Mechanical Physics Solids, Vol. 1, No. 8, 2007, pp. 19–30.

[3] Chang-Kyun, O., Yun-Jae, K., Jong-Hyun, B., Young –Pyo, K. and Woosik, K., "A phenomenological model of ductilefracture for API X65 steel", International Journal of Mechanical Sciences, Vol. 45, No. 10, 2007, pp. 1399–1412.

[4] Narayanasamy, R., and Sathiya Narayanan, C., "Some aspects on fracture limit diagram developed for different steel sheets", Journal of Material Sciences Engineering, Vol. 417, No. 5, 2006, pp. 197–224.

[5] Khelifa, M., Oudjene, M. and Khennane, A., "Fracture in sheet metal forming:effect of ductile damage evolution", Journal of Computers and Structures, Vol, 85. No. 11, 2007, pp. 205–212.

[6] Pickett, A., Pyttel, T., Payen, F., Lauro, F., Petrinic, N., Werner, H., and Christlein, J., "Failure prediction for advanced crashworthiness of transportation vehicles", International Journal of Impact Engineering, Vol. 30, No. 5, 2004, pp. 853–872.

[7] Young-woong, L., Jeffrwy, C. W. and Tomasz, W., "Fracture prediction of thin plates under hemi-spherical punch with calibration and experimental verification", International Journal of Mechanical Sciences, Vol. 46, No. 6, 2004, pp.751–781.

[8] Hooputra, H., Gese, H., Dell, H. and Werner, H., "A comprehensive failure model for crashworthiness simulation of aluminum extrusions", Int. Journal of crash, Vol. 9, No. 9, 2004, pp. 449–463.

[9] Haji Aboutalebi, F., Farzin, M. and Loh-Mousavi, M., "Prediction of rupture in tube hydro-forming process using ductile damage", Int. Journal of Technology of Plasticity, Vol. 9, No. 9, 2008, pp. 125–131.

[10] Kashani, H. and Mosavi, M., "Finite element simulation and experiment in tube hydroforming of unequal T shapes", Journal of Materials Processing Technology, Vol. 177, No. 11, 2006, pp. 684–687.

[11] Hwang, Y. M., Lin, T. C. and Chang, W. C., "Experiment on T-shape hydroforming with counter punch", Journal of Materials Processing Technology, Vol. 192, 193, No. 6, 2007, pp. 243–248.

[12] Imaninejad, M., Subhash, G. and Loukus, A., "Loading path optimization of tube hydroforming process", Journal of Machine Tools and Manufacture, Vol. 45, No. 9, 2005, pp. 1504–1514.

[13] Imaninejad, M., Subhash, G. and Loukus, A., "Influence of end-conditions during tube hydroforming of aluminum extrusions", Journal of Mechanical Science, Vol. 46, No. 8, 2004, pp. 1195–1212.

[14] Johnson, K. I., Nguyen, B. N., Davies, R. W., Grant, G. J. and Khaleel, M. A., "A numerical process control method for circular tube hydroforming prediction", Int. journal of Plasticity, Vol. 201, No. 14, 2004, pp. 1111–1137.

[15] Jansson, M., Nilsson, L. and Simonsson, K., "On constitutive modeling of aluminum alloys for tube hydroforming applications", Int. Journal of Plasticity, Vol. 21, No. 3, 2005, pp. 1041–1058.

[16] Ngaile, G., Jaeger, S. and Altan, T., "Lubrication in tube hydroforming (THF) part II. Performance evaluation of lubricants using LDH test and pear-shaped tube expansion test", Journal. of Materials Processing Technology, Vol. 146, No. 8, 2004, pp. 116–123.

[17] Yuan, S., Qi, J. and He, Z., "An experimental investigation into formability of hydroforming 5A02Al-tubes at elevated temperature", Journal of Materials Processing Technology, Vol. 177, No. 7, 2006, pp. 680–683.

[18] Song, W. J., Kim, J. and Kang, B. S., "Experimental and analytical evaluation on flow stress of tabular material for tube hydroforming simulation", Journal. of Materials Processing Technology, Vol. 46, No. 2, 2007, pp. 368–371.

[19] Ray, P. and Mac Donald, B. J., "Determination of the optimal load path for tube hydroforming process using a fuzzy load control algorithm and finite element analysis", Journal of Finite Element in Analysis and Design, Vol. 41, No. 4, 2004, pp. 173–192.

[20] Manabe, K., Suetake, M., Koyama, H. and Yang, M., "Hydroforming process optimization of aluminum alloy tube using intelligent control technique", Journal of Machine Tools and Manufacture, Vol. 46, No. 8, 2006, pp. 1207–1211.

[21] Yuan, S. J., Han, C. and Wang, X. S., "Hydroforming of automotive structural components with rectangular-sections", Journal of Machine Tools and Manufacture, Vol. 46, No. 4, 2006, pp. 1201–1206.